Regularity Properties of Critical Invariant Circles of Twist Maps, and Their Universality

Arturo Olvera[1*]   Nikola P. Petrov[2†]

August 29, 2006

[1] IIMAS-UNAM, FENOMEC, Apdo. Postal 20–726, México D. F. 01000, Mexico

[2] Department of Mathematics, University of Oklahoma, Norman, OK 73019, USA

Abstract

We compute accurately the golden critical invariant circles of several area-preserving twist maps of the cylinder. We define some functions related to the invariant circle and to the dynamics of the map restricted to the circle (for example, the conjugacy between the circle map giving the dynamics on the invariant circle and a rigid rotation on the circle). The global Hölder regularities of these functions are low (some of them are not even once differentiable). We present several conjectures about the universality of the regularity properties of the critical circles and the related functions. Using a Fourier analysis method developed by R. de la Llave and one of the authors, we compute numerically the Hölder regularities of these functions. Our computations show that – withing their numerical accuracy – these regularities are the same for the different maps studied. We discuss how our findings are related to some previous results: (a) to the constants giving the scaling behavior of the iterates on the critical invariant circle (discovered by Kadanoff and Shenker); (b) to some characteristics of the singular invariant measures connected with the distribution of iterates. Some of the functions studied have pointwise Hölder regularity that is different at different points. Our results give a convincing numerical support to the fact that the points with different Hölder exponents of these functions are interspersed in the same way for different maps, which is a strong indication that the underlying twist maps belong to the same universality class.

[*]E-mail: `aoc@uxmym1.iimas.unam.mx`
[†]E-mail: `npetrov@ou.edu`

Area-preserving twist maps of the cylinder are popular models of the dynamics of many physical systems, i.e., they occur as Poincaré maps of 2-degree-of-freedom Hamiltonian systems. Homotopically non-trivial invariant circles of such a map play an important role in organizing the global dynamics of the map. Generally, as the perturbation grows, more and more of these circles are destroyed, until there remains only one such circle, called the "critical" circle. This circle is the last obstacle to the unbounded growth of the "action variable". In this critical situation many characteristics of the system become drastically different from the "under-critical" case. For example, consider the dynamics of the iterates of the twist map restricted to the critical circle – it is given by a map of the circle. This map can be conjugated to a rigid rotation on the circle, but the conjugating function has very low regularity – its Hölder exponent is lower than 1. The Hölder regularity of this conjugacy is related to some universal properties of the map, i.e., to the universal rescaling factors [1, 2] and to the scaling properties [3] of the distribution of the iterates on the critical circle (which is governed by a singular invariant measure). We compute several functions related to the critical circle and to the dynamics on it and us a method developed in [4] to assess numerically their global Hölder regularity. Our findings lend support to several conjectures concerned with the universality and the renormalization group description of these critical objects.

1   Introduction

It has been known since the late 1970's and early 1980's that many objects at the boundary of chaotic behavior exhibit remarkable scaling properties and that, furthermore, these properties are "universal". Such properties are exhibited by unimodal maps of the interval [5, 6, 7], critical maps of the circle [8], critical KAM tori [1, 2], and other systems. These observations were explained in terms of a renormalization group analysis, following a methodology that had been developed earlier in the study of critical phenomena in statistical mechanics and field theory [9, 10, 11, 12].

The scale invariance of the critical objects affects many of their properties. Notably, the Hölder regularity of the critical objects (or some functions related to them) tends to have a low and fractional value. Presumably the values of the regularities are related to exponents and geometric properties of the renormalization group fixed points which describe the critical objects.

Furthermore, the observation that critical objects can be divided in "universality classes" such that all objects in a given class "look the same" can be tested numerically. One way to do this is to define certain functions related to the critical objects – typically these functions are not very regular (in some cases not even once differentiable), and to test numerically whether the regularities of these functions are the same for different objects. Another – even more sensitive – test for universality is to take two functions, say h_1 and h_2, from the same

2

class, and to study the regularity of functions like $h_1 \circ h_2^{-1}$ – for h_1 and h_2 belonging to the same universality class, one can expect that $h_1 \circ h_2^{-1}$ be more regular than h_1 and h_2^{-1}. These ideas were tested in [4] in the case of non-critical and critical (with different degree of criticality) circle maps, in which the empirical results are accompanied by an extensive mathematical theory. A substantial part of the effort in [4] was to develop implementations of methods known in harmonic analysis (finite differences, Littlewood-Paley theory, wavelet analysis) to assess the regularity of the objects numerically.

In the present paper, we extend the methodology of [4] to the study of critical invariant circles of area-preserving twist maps. Invariant circles in dynamical systems are among the most important objects that organize the long-term behavior of the system, and the critical ones are especially important because of their role as "last barriers to chaos" (for readable reviews see, e.g., [13], or, with more emphasis on the mathematical aspects, the recent book [14]). Critical invariant circles have been extensively studied since early 1980's [1, 2, 15, 12].

We compute accurately the golden critical invariant circles of several standard-like area-preserving twist maps and some functions related to the dynamics of the iterates of the maps on these circles. Then we apply methods developed in [4] to study the Hölder regularity of these functions and some universality aspects.

In Sec. 2 we give some background on twist maps and their critical invariant circles, define the functions that are the objects of our numerical study, and present several precise conjectures concerning the properties of the critical invariant circles and the functions introduced. Sec. 3 is devoted to a discussion of the numerical methods used to compute critical invariant circles and to assess Hölder regularity of functions. We collect our results in Sec. 4, and in Sec. 5 we discuss their significance and relationship with previous studies.

2 Critical invariant circles of twist maps

2.1 Twist maps

Let $\mathbb{T} := \mathbb{R}/\mathbb{Z}$ stand for the circle. We will be concerned with maps F of the (infinite) cylinder $\mathbb{T} \times \mathbb{R}$,

$$F : \mathbb{T} \times \mathbb{R} \to \mathbb{T} \times \mathbb{R} : (\theta, r) \mapsto F(\theta, r) =: (\theta', r') \,,$$

which satisfy the following properties:

- *Area preservation:* The map F preserves the oriented area: $\det DF = 1$.

- *Zero-flux:* The oriented area between a homotopically non-trivial circle and its image under F is 0. (In our situation, this is equivalent to saying that every non-trivial circle intersects its image.)

- *Twist condition:* For any fixed value of θ, $\frac{\partial \theta'}{\partial r} > 0$.

A map of the cylinder can be identified with a map $\tilde{F} : \mathbb{R}^2 \to \mathbb{R}^2$ (called a *lift* of F) which satisfies

$$\tilde{F}(\theta + 1, r) = \tilde{F}(\theta, r) + (1, 0) \ .$$

Often one does not need to keep the distinction.

The maps which we will use in our numerical studies are of the form $(\theta', r') := F(\theta, r)$ with

$$
\begin{aligned}
\theta' &= (\theta + r') \bmod 1 \ , \\
r' &= r + \lambda V(\theta) \ ,
\end{aligned}
\tag{1}
$$

where λ is a parameter, and $V : \mathbb{T} \to \mathbb{R}$ is a function satisfying $\int_0^1 V(\theta)\, d\theta = 0$. In particular, many numerical studies have been devoted to studying (1) with

$$V(\theta) = -\frac{1}{2\pi} \sin 2\pi\theta \ , \tag{2}$$

in which case we will call the map F the *Taylor-Chirikov* map.

Given an orbit $\mathcal{X} = \{(\theta_n, r_n) = F^n(\theta_0, r_0) \,|\, n = 0, 1, 2, \ldots\}$, we define its *rotation number*, $\rho(\mathcal{X})$, as the limit

$$\rho(\mathcal{X}) := \lim_{n \to \pm\infty} \frac{\theta_n - \theta_0}{n} \ ,$$

whenever this limit exists. In contrast with the situation for circle maps, the rotation number depends on the orbit (and it may happen that some orbits do not have rotation number).

We say that an orbit is *well-ordered* when for every k and l, the function of n defined as $e(n) = \theta_{n+k} - l - \theta_n$ has the same sign. Every well-ordered orbit has a rotation number (the converse, however, is not true).

It is also easy to see that if a bounded orbit is well-ordered and $\rho(\theta_0, r_0)$ is irrational, the closure of the orbit, $\overline{\{(\theta_n, r_n)\}_{n=0}^\infty}$, is a perfect set (i.e., every point is an accumulation point of points in the set); in other words, in this case the orbit is either a homotopically non-trivial circle or a Cantor set.

A set $U \subseteq \mathbb{T} \times \mathbb{R}$ is *invariant* if $U = F(U)$.

The following result plays an important role.

Theorem 2.1. *If F is as above, for every $\rho \in \mathbb{R}$ there exists a well-ordered orbit with rotation number ρ.*

2.2 Invariant circles of twist maps – rigorous results

The proof of the following theorem can be found in [16], [17]. We refer to [14] and [18] for a detailed exposition.

Theorem 2.2. *Let U be an open simply connected invariant set, containing one of the ends of the cylinder. Then the boundary, ∂U, of the set U is an invariant circle which is the graph*

4

of a Lipschitz function. In other words, ∂U can be written as $r = R(\theta)$, where $R : \mathbb{T} \to \mathbb{R}$ is a Lipschitz function.

For the map (1), the Lipschitz constant of the function R can be bounded by an expression which involves only the Lipschitz constant of the function F in a neighborhood of the circle ∂U.

In particular,

Corollary 2.1. *Any homotopically non-trivial invariant circle is the graph of a Lipschitz function R. In the particular case of the map* (1), *the Lipschitz constant of R can be bounded by a constant which is independent of $\lambda \operatorname{Lip} V$.*

A number ρ is said to be *Diophantine* if, for each $m, n \in \mathbb{N} \setminus \{0\}$, for some $C > 0$, and for some $d > 2$, it satisfies

$$\left| \rho - \frac{m}{n} \right| > \frac{C}{n^d} \ .$$

In the case when the map F is close to integrable and its rotation number ρ is Diophantine, one can apply Kolmogorov-Arnold-Moser theory to obtain that there exists an analytic invariant circle such that the orbits on it have rotation number ρ.

Golden invariant circles are those with rotation number equal to the *golden mean*,

$$\sigma_G := [1, 1, 1, \ldots] = \frac{\sqrt{5} - 1}{2} \ . \tag{3}$$

Here we have used the notation $\rho = [a_1, a_2, a_3, \ldots] = 1/(a_1 + 1/(a_2 + 1/(a_3 + \cdots)))$ for the continued fraction expansion of $\rho \in (0, 1)$ [19].

There are also rigorous results that guarantee the non-existence of invariant circles of F of the form (1).

Theorem 2.3. *(i) If $\sup_\theta |\lambda V(\theta)| > 1$, then* (1) *has no invariant circles.*

(ii) If $\sup_\theta |V'(\theta)| = 1$ (which holds for the function (2)*), then for $|\lambda| > \frac{4}{3}$ the map* (1) *has no invariant circles.*

(iii) For V given by (2)*, the map* (1) *has no golden invariant circles for $|\lambda| > \frac{63}{64} = 0.984375\ldots$.*

(iv) For V given by (2)*, the map* (1) *has no golden invariant circles for $|\lambda| > 0.9718$.*

Part (i) of Theorem 2.3 is elementary: if $\lambda \sup_\theta |V(\theta)| > 1$, then there will exist points $(\theta^*, r^*) \in \mathbb{T} \times \mathbb{R}$ such that $F(\theta^*, r^*) = (\theta^*, r^* + 1)$, which, iterated, gives that $F^n(\theta^*, r^*) = (\theta^*, r^* + n)$ – the unbounded growth of the second coordinate of $F^n(\theta^*, r^*)$ with n implies that a topologically non-trivial invariant circle cannot exist.

Part (ii) can be found in [17], parts (iii) and (iv) are proved by computer-assisted methods in [20] and [21], resp.

It is widely believed that

5

Conjecture 2.1. *For a Diophantine number ρ and for a map F of the form* (1)*, there is a number $\Lambda(\rho)$ such that when $|\lambda| > \Lambda(\rho)$, there is no invariant circle with rotation number ρ, and when $|\lambda| < \Lambda(\rho)$, there exists an analytic invariant circle with rotation number ρ. The invariant circle becomes critical when $|\lambda| = \Lambda(\rho)$.*

Since our paper is devoted to homotopically non-trivial invariant circles, we will usually omit the words "homotopically non-trivial".

2.3   Functions related to the critical invariant circles

We are interested in describing the critical invariant circles with rotation number ρ which are in the boundary of existence. Postponing for the moment issues on how these objects can be actually computed, we point out that to a given critical invariant circle γ of rotation number ρ, we can associate:

- the function $R : \mathbb{T} \to \mathbb{R}$ such that the critical invariant circle γ is the graph of R:

$$\gamma = \{(\theta, r) \in \mathbb{T} \times \mathbb{R} \, : \, r = R(\theta)\} \; ; \tag{4}$$

- the *advance map* $g : \mathbb{T} \to \mathbb{T}$ defined by

$$F(\theta, R(\theta)) = (g(\theta), R \circ g(\theta)) \; ; \tag{5}$$

- the *hull map* $\Psi : \mathbb{T} \to \mathbb{T} \times \mathbb{R}$, which gives a representation of the invariant circle γ in such a way that the dynamics on γ becomes a rotation by ρ, i.e.,

$$F \circ \Psi(\theta) = \Psi(\theta + \rho) \; ; \tag{6}$$

- the map $h = \pi_1 \circ \Psi : \mathbb{T} \to \mathbb{T}$ (where $\pi_1 : \mathbb{T} \times \mathbb{R} \to \mathbb{T}$ is the projection onto $\mathbb{T}$), which conjugates the advance map to a rotation by ρ:

$$g \circ h(\theta) = h(\theta + \rho) \; ; \tag{7}$$

- the map $h^{-1} : \mathbb{T} \to \mathbb{T}$, which is the inverse of the map h defined in (7).

We note the following rigorous results.

Theorem 2.2 guarantees that the invariant circle the function R is Lipschitz. It is an easy consequence of the implicit function theorem that g should be as regular as R. Nevertheless, it is useful to compute the regularities of both g and R independently to asses the reliability of the numerical methods used.

Because of (7), it is clear that the regularity of g is not smaller than the minimum of the regularities of h and h^{-1}.

6

2.4 The "big" conjugacies

Let ρ be a Diophantine number, F_i ($i = 1, 2$) be area-preserving twist maps, and γ_i be the critical invariant circle of F_i with rotation number ρ. Let g_{γ_i} and h_{γ_i} be the associated advance map (5) and conjugacy (7), resp. We introduce the conjugating functions

$$G_{\gamma_1,\gamma_2} := g_{\gamma_1} \circ g_{\gamma_2}^{-1} : \mathbb{T} \to \mathbb{T} \ ,$$

$$H_{\gamma_1,\gamma_2} := h_{\gamma_1} \circ h_{\gamma_2}^{-1} : \mathbb{T} \to \mathbb{T} \ .$$

We will call these functions "big" conjugacies to distinguish them from the "small" conjugacies h that conjugate the projected dynamics on the critical circles to a rigid rotation (7). Note that the "big" conjugacies satisfy

$$G_{\gamma_1,\gamma_2} \circ G_{\gamma_2,\gamma_3} = G_{\gamma_1,\gamma_3} \ , \quad H_{\gamma_1,\gamma_2} \circ H_{\gamma_2,\gamma_3} = H_{\gamma_1,\gamma_3} \ .$$

Below we discuss one aspect of the definition of the big conjugacies that will be important in our computations.

Since there is no "origin" on the circle $\mathbb{T}$, one has certain amount of freedom in the definition of some maps. For example, if the function Ψ is a hull map (i.e., satisfies (6)), then the function $\tilde{\Psi}$ defined as $\tilde{\Psi}(\theta) = \Psi(\theta + \zeta)$ will also satisfy (6) for any choice of the constant ζ. Similarly, the map h (7) that conjugates the advance map g to a rigid rotation can be redefined by composing it on the right with a rotation, and the resulting map, $\tilde{h}(\theta) = h(\theta + \zeta)$, will also conjugate g to a rigid rotation. Naturally, all important properties of the maps h and $\tilde{h}$ – in particular, their Hölder regularity – will be the same. However, one cannot use this freedom liberally when studying the big conjugacies. To understand the reason for this, consider the map h defined by (7) for some twist map F. Naturally, the map $h \circ h^{-1}$ is the identity map, so it is C^∞. However, for any nonzero ζ in the definition of $\tilde{h}$, there is no guarantee that the map $h \circ \tilde{h}^{-1}$ will be C^∞. This is due to the fact that the regularity of h may be different at different points, and while in $h \circ h^{-1}$ these "irregularities" cancel out, in $h \circ \tilde{h}^{-1}$ the action of h does not necessarily "undo" the irregularities caused by $\tilde{h}^{-1}$. In Sec. 2.5 we explain in detail how we choose ζ in order to avoid the "spurious" irregularities of the big conjugacy.

2.5 Big conjugacies and symmetries

Consider two functions h_{γ_1} and h_{γ_2} corresponding to the critical circles γ_1 and γ_2 of the twist maps F_1 and F_2. If F_1 and F_2 happen to belong to the same "universality class" (see Sec. 2.6), then one would expect that the big conjugacy H_{γ_1,γ_2} will be more regular than the functions h_{γ_1} and $h_{\gamma_2}^{-1}$. To avoid introducing spurious irregularities in H_{γ_1,γ_2}, we use the symmetries of the map h that come from the symmetries of the F [22, 23, 24].

It is well known that if the function V is odd, then the map F given by (1) can be written as a composition of two involutions:

$$F = I_1 \circ I_0 \ , \qquad I_0^2 = I_1^2 = \text{Id} \ , \tag{8}$$

where
$$I_0(\theta, r) = (-\theta, r + \lambda V(\theta)) , \quad I_1(\theta, r) = (-\theta + r, r) . \tag{9}$$

From (8) we have $I_0 \circ F = F^{-1} \circ I_0$ and $I_1 \circ F = F^{-1} \circ I_1$. Acting on (6) with I_0 from the left, we obtain
$$F^{-1} \circ (I_0 \circ \Psi)(\theta) = (I_0 \circ \Psi)(\theta + \rho) . \tag{10}$$

On the other hand, if we define the function $L : \mathbb{T} \to \mathbb{T} \times \mathbb{R}$ by $L(\theta) := \Psi(-\theta)$, then (6) can be written as
$$F^{-1} \circ L(\theta) = L(\theta + \rho) . \tag{11}$$

Comparing (10) and (11), we see that L and $I_0 \circ \Psi$ can differ only by a shift in the argument, i.e., there has to exist a constant ζ such that $I_0 \circ \Psi(\theta) = L(\theta + \zeta) = \Psi(-\theta - \zeta)$. This, together with (9) and $h = \pi_1 \circ \Psi$, imply

$$h(\theta) = -h(-\theta - \zeta) .$$

This implies that $h(-\frac{\zeta}{2}) = 0$, and the numerical value of ζ can be found from the computed values of h. Setting $\tilde{h}(\theta) := h(\theta - \frac{\zeta}{2})$, we obtain that $\tilde{h}$ is an odd function. In what follows, we will assume that the appropriate value of ζ has been subtracted, and will omit the tilde over h.

2.6 Universality

In this section, we formulate precisely some conjectures on the behavior of critical invariant circles described by a non-trivial fixed point of the renormalization group. It seems quite possible that these conjectures can be proved as conditional theorems assuming existence and certain properties of this fixed point.

One of the most striking predictions of the renormalization group theory is that many characteristics of the critical invariant circles are largely independent of the details of the map. This is captured by the notion of universality.

Definition 2.1. *We say that a numerical characteristic is* universal *when it takes the same value in an open set of functions. We say that a property is* universal *when it holds for an open set of functions.*

The open sets alluded to in Definition 2.1 are called *domains of universality*.

For the case that we will be concerned with, the description of the domains of universality in terms of properties of the non-trivial fixed points of the renormalization operator is still debated, but there are indications that the domain of universality is not the whole space [25, 26, 27].

Conjecture 2.2. *The existence of one and only one non-trivial fixed point of the renormalization operator is a universal property.*

This conjecture has been known for a long time [12]. Recently in [28] it has been shown how this conjecture follows rigorously from an extension of the standard renormalization group picture. Even the formulation of the subsequent conjectures depends of Conjecture 2.2.

The concept of universality is rather natural when one wants to study properties that depend on the speed at which the set of maps converges to the fixed point under the renormalization operator. In particular, regularity of conjugacies depends on the this speed of convergence and, hence, should be a universal quantity (more precise formulations are given in [29]). Hence, we can also conjecture that:

Conjecture 2.3. *The regularity, $\kappa(R)$, of the critical invariant circle is a universal number.*

Conjecture 2.4. *The regularities $\kappa(g)$, $\kappa(h)$ and $\kappa(h^{-1})$ are universal numbers.*

Conjecture 2.5. *For pairs of critical circles γ_1 and γ_2, the regularities $\kappa(G_{\gamma_1,\gamma_2})$ and $\kappa(H_{\gamma_1,\gamma_2})$ are universal numbers.*

Directly from the definition of Hölder regularity, one can see that if $\kappa(\phi)$ and $\kappa(\psi)$ are between 0 and 1, then $\kappa(\phi \circ \psi) \geq \kappa(\phi)\,\kappa(\psi)$. This implies that

$$\kappa(H_{\gamma_1,\gamma_2}) = \kappa(h_{\gamma_1} \circ h_{\gamma_2}^{-1}) \geq \kappa(h_{\gamma_1})\,\kappa(h_{\gamma_2}^{-1})\;. \tag{12}$$

For all critical invariant circles γ_i that we studied, we obtained numerically that $\kappa(h_{\gamma_i}) < 1$ and $\kappa(h_{\gamma_i}^{-1}) < 1$, so (12) yields that H_{γ_1,γ_2} is not less regular than $\kappa(h_{\gamma_1})\,\kappa(h_{\gamma_2}^{-1})$. For γ_1 and γ_2 in the same universality class, however, we expect more – because of "cancellation" of the "singularities" of h_{γ_1} and $h_{\gamma_2}^{-1}$, we state our final

Conjecture 2.6. *The following inequalities hold for $i = 1, 2$:*

$$\kappa(h_{\gamma_i}) < \kappa(H_{\gamma_1,\gamma_2})\;, \qquad \kappa(h_{\gamma_i}^{-1}) < \kappa(H_{\gamma_1,\gamma_2})\;.$$

3   Description of the numerical methods

In this section we first describe the methods used for numerical computation of invariant circles and the related functions described in Sections 2.3 and 2.4. Then we briefly discuss the method we use to compute the global Hölder regularity of the functions.

3.1   Computing critical invariant circles

We need to compute (homotopically non-trivial) critical invariant circles of twist maps of the form (1) with a Diophantine rotation number. We approximate such invariant circles by well-ordered periodic orbits (whose existence is guaranteed by the so-called Birkhoff's Geometric Theorem [30]). Consider a sequence $\{\mathcal{X}^{(j)}\}_{j \in \mathbb{N}}$ of well-ordered periodic orbits whose rotation numbers, $\{\rho_j\}_{j \in \mathbb{N}}$, constitute a sequence of rational numbers which converge to a Diophantine number ρ. Then the limit of these periodic orbits will be a well-ordered invariant set $\mathcal{X}_\rho$ of rotation number ρ; the existence of this set is guaranteed by Aubry-Mather

theory [31, Ch. 13], [14, Ch. 2]. The set $\mathcal{X}_\rho$ can be a continuous curve which is a graph of a Lipschitz function under appropriate conditions (Theorem 2.2) or an orbit homeomorphic to a Cantor set (Cantorus).

We approximate a Diophantine number ρ by the rational numbers given by finite truncations of the continued fraction expansion of ρ. In the case of the golden mean σ_G (3), these rational approximants are ratios $\rho_m = Q_{m-1}/Q_m$ of consecutive Fibonacci numbers Q_m. The limit of the periodic orbits with rotation numbers ρ_m is the invariant set $\mathcal{X}_\rho$ we are looking for [23].

The problem of computing well-ordered orbits with a prescribed rational rotation number ρ_m is greatly simplified if the function $V(\theta)$ in (1) is odd. In this case the task of finding a periodic orbit is reduced to a one-dimensional problem because the map F can be written as the composition of two involutions as in (8); if such a decomposition is possible, the map F is said to be *reversible*. If F is reversible, there exists a set of straight lines in the (θ, r) space – called *symmetry lines* – that are invariant with respect to the maps I_0 and I_1. It can be shown that any periodic orbit has two points that belong to one of these invariant straight lines, hence we can find these points (and, therefore, the periodic orbits that contain them) by using a one dimensional root finder [23]. Using the fact that the periodic orbits computed in this way are well-ordered, we can implement a numerical procedure to compute periodic orbits of several million points that approximate the invariant set $\mathcal{X}_\rho$.

We are interested in studying the properties of area-preserving twist maps of the form (1). When the parameter λ in (1) is equal to 0, the corresponding twist map acts on each point (θ, r) as a rigid rotation in θ-direction, $F(\theta, r) = (\theta + r, r)$, hence the phase space is foliated by invariant circles of the form $\{r = \text{const}\}$. For small values of $|\lambda|$, KAM theory guarantees the existence of invariant circles with Diophantine rotation numbers. According to Conjecture 2.1, there is an upper bound $\Lambda(\rho)$ on the values of $|\lambda|$ such that for $|\lambda| < \Lambda(\rho)$ there exists an invariant circle with rotation number ρ; (some rigorous upper bounds on $\Lambda(\rho)$ are given in Theorem 2.3). To find an accurate numerical approximation of the critical value, $\Lambda(\rho)$, of λ for which the invariant circle of rotation number ρ disintegrates, we applied an empirical method known as the "residues method" proposed in [23], developed in [32], and partially justified rigorously in [33]. The main idea of this method is to determine the value of λ such that the residue of all the approximating periodic orbits reaches the same value. Let R_m be the residue of a periodic orbit which is the mth approximant to an invariant circle with rotation number ρ. If $\lim_{m\to\infty} R_m = 0$, then there exists an invariant circle with rotation number ρ; if $\lim_{m\to\infty} R_m = \infty$, then the invariant set $\mathcal{X}_\rho$ becomes a Cantor set. A golden critical invariant circle is obtained at the value of λ for which $R_m \simeq -2.55426$ for all values of m.

3.2   Studying global Hölder regularity numerically

In this section we describe briefly the method we employed to study global Hölder regularity, referring the reader to [4] for details, references, and assessment of the numerical accuracy of various numerical methods for computing regularity.

In this paper, we will only use the method developed in [4] that was found to be the most

accurate for studying global Hölder regularity – the so-called "Continuous Littlewood-Paley" (CLP) method. Here we do not use the wavelet-based methods implemented in [4]. The CLP method has been used in [34, 24].

3.2.1 Theoretical basis of the CLP method

We recall the following definition.

Definition 3.1. *For $\kappa = n + \chi$ with $n \in \mathbb{Z}$, $\chi \in (0,1)$, we say that the function $K : \mathbb{T} \to \mathbb{R}$ has (global) Hölder exponent κ and write $K \in \Lambda_\kappa(\mathbb{T})$ when K is n times differentiable and, for some constant $C > 0$,*

$$|D^n K(\theta) - D^n K(\tilde{\theta})| \leq C|\theta - \tilde{\theta}|^\chi$$

for all $\theta, \tilde{\theta} \in \mathbb{T}$.

For the case of an integer value of κ, this definition is more complicated, but we will omit it since in the applications considered in this paper κ is not an integer.

The following result can be found in [35, Ch. 5, Lemma 5].

Theorem 3.1 (CLP). *The function $K \in L^\infty(\mathbb{T})$ is in $\Lambda_\kappa(\mathbb{T})$ if and only if for some integer $\eta > \kappa$ there exists a constant $C > 0$ such that for any $t > 0$*

$$\left\| \left(\frac{\partial}{\partial t} \right)^\eta e^{-t\sqrt{-\Delta}} K \right\|_{L^\infty(\mathbb{T})} \leq C t^{\kappa - \eta}, \tag{13}$$

where Δ is the one-dimensional Laplace operator: $\Delta K(\theta) = K''(\theta)$.

Remark 3.1. If the above result holds for some integer $\eta > \alpha$, then it holds for all integers $\tilde{\eta} > \alpha$.

Remark 3.2. The operator $e^{-t\sqrt{-\Delta}}$ is a convolution with the Poisson kernel: $e^{-t\sqrt{-\Delta}}K = P_{\exp(-2\pi t)} * K$. The function $u(\theta, t) := e^{-t\sqrt{-\Delta}}K(\theta)$ is a solution of Laplace's equation, $u_{\theta\theta} + u_{tt} = 0$, on the half-cylinder $(\theta, t) \in \mathbb{T} \times (0, \infty)$, with Dirichlet boundary condition $u(\theta, 0) = K(\theta)$.

Remark 3.3. The mathematical theory only requires that (13) be an upper bound. In our numerical experiments, however, this bound is saturated for a significant range of values of t. This fact is very possibly a consequence of the self-similarity at small scales of the functions we consider (which is at the basis of the renormalization group description). This saturation was also observed for the functions considered in [4, 24].

3.2.2 Remarks on the numerical implementation

To use the CLP method, we need to apply repeatedly Fast Fourier Transform (FFT), which is easiest to do if the values of the function K in (13) are known at 2^N equally spaced points in the interval $[0,1)$ for some positive integer N. However, as we describe in Sec. 4, we do not have control over the set of points at which the values of K can be computed (where K stands for any of the functions R, g, h, h^{-1}, H, G). Hence, the first step in applying the CLP method would be the computation of the values of K on an evenly spaced grid. If we know accurately the values of K at M points in $[0,1)$, we can expect that by using some interpolation method, we will be able to obtain the approximate values of K on $2^N \approx M$ equidistant points, $\{2^{-N}j\}_{j=0}^{2^N-1}$. To compute the approximate values of K on the equidistant grid, we used cubic spline interpolation. Using interpolation poses the question of whether the interpolated values represent faithfully the true values of K. Naturally, the answer to this question is no, but practically if M is large enough, the interpolated values will be very close to the true values, which will allow us to compute many Fourier coefficients of K accurately. The degree of "contamination" of the Fourier spectra due to the interpolation depends on the uniformity of the distribution of the M points at which the values of K is known accurately (see Remark 4.2).

To apply the CLP method numerically, we observe that the operator $\left(\frac{\partial}{\partial t}\right)^\eta e^{-t\sqrt{-\Delta}}$ used in Theorem 3.1 is diagonal in a Fourier series representation: if $K(\theta) = \sum_{k\in\mathbb{Z}} \hat{K}_k e^{-2\pi i k\theta}$, then

$$\left(\frac{\partial}{\partial t}\right)^\eta e^{-t\sqrt{-\Delta}} K(\theta) = \sum_{k\in\mathbb{Z}} (-2\pi|k|)^\eta\, e^{-2\pi t|k|}\, \hat{K}_k\, e^{-2\pi i k\theta} \ . \tag{14}$$

Having computed the values of the spline interpolant to the function K on an equally spaced grid, applying (13) is easy. Namely, we fix some values of the parameters η and t, perform FFT to find $\hat{K}_k$ and compute the Fourier coefficients of $\left(\frac{\partial}{\partial t}\right)^\eta e^{-t\sqrt{-\Delta}} K$. Then we apply inverse FFT to find the values of $\left(\frac{\partial}{\partial t}\right)^\eta e^{-t\sqrt{-\Delta}} K$ at the equally spaced set of points $\{2^{-N}j\}_{j=0}^{2^N-1}$; among these values we find the one with maximum absolute value – this value we take for the numerical value of the left-hand side of (13). For a fixed value of η, we repeat this procedure for many values of t (we used several hundred values of t in our computations). According to (13), if we plot

$$\log \left\| \left(\frac{\partial}{\partial t}\right)^\eta e^{-t\sqrt{-\Delta}} K \right\|_{L^\infty(\mathbb{T})} \qquad \text{versus} \quad \log t \ , \tag{15}$$

the points should lie below a straight line of slope $\kappa - \eta$. As pointed out in Remark 3.3 (see also Remark 4.3) the points on the log-log plot should not only be below this straight line, but should close to it. We perform linear regression to find the slope of this line, from which we find κ.

4 Numerical results

4.1 Twist maps studied

We study numerically a set of one-parameter families of area-preserving twist maps of the form (1), each family having a different function V. Within each family we find numerically the value $\Lambda(\sigma_{\mathrm{G}})$ of the parameter λ for which the golden invariant circle is critical. The set of functions V (all of them odd) that we selected is the following:

1. The standard (Taylor-Chirikov) map:

$$V_1(\theta) = -\frac{1}{2\pi} \sin 2\pi\theta \ . \tag{16}$$

2. The "standard map with two harmonics":

$$V_2(\theta) = -\frac{1}{2\pi} \left[\sin(2\pi\theta) - 0.03 \sin(6\pi\theta)\right] \ . \tag{17}$$

3. The "critical standard map with two harmonics":

$$V_3(\theta) = -\frac{1}{2\pi} \left[\sin(2\pi\theta) - \frac{1}{2}\sin(6\pi\theta)\right] \ . \tag{18}$$

   For this choice of coefficients, the first three derivatives of $V(\theta)$ at $\theta = 0$ are zero.

4. The "0.2-analytic map":

$$V_4(\theta) = -\frac{1}{2\pi}\frac{\sin(2\pi\theta)}{1 - 0.2\cos(2\pi\theta)} \ . \tag{19}$$

   This map has infinitely many nonzero Fourier coefficients. It would be very interesting to study this map when the coefficient of the cosine function in the denominator is close to 1, but then it would be extremely difficult to compute periodic orbits.

5. The "0.4-analytic map":

$$V_5(\theta) = -\frac{1}{2\pi}\frac{\sin(2\pi\theta)}{1 - 0.4\cos(2\pi\theta)} \ . \tag{20}$$

6. The "tent map":

$$V_6(\theta) = \sum_{j=1}^{17} c_j \sin(2\pi j\theta) \ , \tag{21}$$

   where $c_j = (-1)^{\frac{j+1}{2}}\frac{4}{\pi^2 j^2}$ for j odd, and $c_j = 0$ for j even, are the Fourier coefficients of the function

$$\mathcal{V}(\theta) = \begin{cases} -4\theta \ , & \text{for } 0 \leq \theta < \frac{1}{4} \ , \\ 4\theta - 2 \ , & \text{for } \frac{1}{4} \leq \theta < \frac{3}{4} \ , \\ 4 - 4\theta \ , & \text{for } \frac{3}{4} \leq \theta < 1 \ . \end{cases}$$

   The function V_6 is close to the piecewise linear continuous function $\mathcal{V}$.

13

Our numerical experiments were performed with the twist maps coming from the above six functions $V(\theta)$ and the corresponding values $\Lambda(\sigma_G)$, following the steps below.

1. As discussed in Sec. 3.1, the invariant circle of rotation number σ_G can be obtained as a limit of periodic orbits of rotation numbers equal to ratios of consecutive Fibonacci numbers, $\rho_m = Q_{m-1}/Q_m$. We chose to compute hyperbolic periodic orbits, and found the values of $\Lambda(\sigma_G)$ by applying Greene's residue criterion.

2. The highest approximant to the critical invariant circle that we computed was a periodic orbit with rotation number $Q_{29}/Q_{30} = 832040/1346269$. The value of $\Lambda(\sigma_G)$ was determined by using the condition that the difference, $|R_{30} - R_{29}|$ of the residues of the periodic orbits with periods Q_{29} and Q_{30} be zero (in practice, we wanted that this difference be smaller than 10^{-10}). The periodic orbits were computed with an error not exceeding 10^{-23}.

3. We computed the hyperbolic periodic orbit $\{(\theta_m, r_m)\}_{m=0}^{M-1}$ of period $M = Q_{30}$. The values of the advance map g (5) at the points θ_m ($m = 0, 1, \ldots, M-1$) were then computed by $g(\theta_m) = \theta_{m+1}$ (here and below, we take mod 1 wherever needed). The values of the conjugacy h at the points $m\sigma_G$ (which corresponds to m applications of the rigid rotation by σ_G to 0) are given by $h(m\sigma_G) = \theta_m$, and, similarly, $h^{-1}(\theta_m) = m\sigma_G$.

4. In our Fourier-analysis-based CLP method we need to deal with periodic functions, so we compute the "periodized" versions, $g - \mathrm{Id}$, $h - \mathrm{Id}$, $h^{-1} - \mathrm{Id}$, of the functions g, h, and h^{-1}. Then we sort the periodized functions with respect to their argument; the function R is already periodic, so we just sort its values.

5. The periodic functions are passed to the cubic spline interpolation routine to find approximations to the values of the corresponding functions on a uniformly spaced grid of 2^N points; we used $N = 20$.

6. The interpolated values of the functions are given to the CLP algorithm to compute their Hölder regularity. We used integer values of η in (13) from 1 to 5, and for each analyzed function chose the value of η that gave the best straight line on the log-log plot (15). The log-log plots for the other values of η were used as a consistency check.

Remark 4.1. In computing the big conjugacies H_{γ_1, γ_2}, we had to take special care of the preserving the symmetries of the maps h. For each critical circle we studied, we needed to find the appropriate value of the constant ζ and shift the argument of the corresponding function h as explained in Sec. 2.5.

4.2   Critical invariant circles – visual explorations

In Fig. 1 we show the critical invariant circles which, by the definition (4), are graphs of the functions R corresponding to the six twist maps studied. The graphs of the "periodized

versions" of the advanced maps, $g - \mathrm{Id}$, the conjugacies, $h - \mathrm{Id}$, and their inverses, $h^{-1} - \mathrm{Id}$, are plotted in Figures 2, 3, and 4, resp.

Figure 5 illustrates the self-similar nature the functions h; needless to say, the insets are true zooms of parts of the graph of the function.

Fig. 6 shows the graphs of several periodized big conjugacies $H - \mathrm{Id}$; it is obvious that these functions are smoother than the "small" conjugacies h.

4.3   Fourier spectra, CLP method

Fig. 7 depicts $\log_{10}$ of the modulus of the kth Fourier coefficient of a periodized conjugacy $(h - \mathrm{Id})$ versus $\log_{10} k$; here h is the conjugacy corresponding to the twist map F with V_3 (18). The horizontal distance between two adjacent high peaks is approximately equal to $|\log_{10} \sigma_\mathrm{G}| \approx 0.209$, which is a manifestation of the self-similarity at small scales. The $\log_{10}$-$\log_{10}$ plots of the Fourier spectra of the functions $(g - \mathrm{Id})$ and $(h^{-1} - \mathrm{Id})$ for the same map F are given in Fig. 8.

Remark 4.2. Note that the spectrum of h is very accurate even at length-scales $\sim 10^{-6}$, while the spectrum of h^{-1} is quite noisy. As explained in Sections 3.2.2 and 4.1, the main reason for this is that the exact values of h are known at the points $(m\sigma_\mathrm{G}) \bmod 1$, which are almost uniformly distributed on $\mathbb{T}$. On the other hand, we know the exact values of of g and h^{-1} at the very nonuniformly distributed points of the form $g^m(\theta_0)$ (because the underlying invariant measure is singular – see Sec. 5.2), which results in the presence of big gaps between these points and, hence, distorted values of the spline interpolant.

In Fig. 9 we show several plots of $\log_{10}$ of the left-hand side of (13) versus $\log_{10} t$. The six lines in each group of lines of similar slope correspond to the six different choices (16)–(21) of functions V, and the lines in each group come from the same value of η in (13). Each on the "lines" in the figure in fact consists of 400 points (visually indistinguishable). The computer time spent on the CLP analysis is of the order of one minute per point (we used 2^{20} Fourier coefficients to compute each of these points).

We computed the regularity by performing linear regression on the points on graphs like the one in Fig. 9, in the regions where the points follow more or less a straight line. As one can see from this figure, for t close to 1 (i.e., $\log_{10} t \approx 0$), the graphs for different functions are not straight lines, then as t decreases they form more or less straight lines, and as t decreases further, these lines level out. This behavior can be understood intuitively from (14) – for $t \approx 1$ the high-k Fourier coefficients are strongly suppressed by the factor $(-2\pi|k|)^\eta \, e^{-2\pi t|k|}$, so the CLP method still does not "feel" the asymptotic self-similarity of the functions at small length-scales; in the other extreme, the leveling-out of the lines for very small t comes from the fact that in our computations we use a finite – albeit very large – number of Fourier coefficients.

Remark 4.3. The "straight lines" in Fig. 9 are not really straight (which has been noticed in different contexts in [4, 24]). We show this effect in Fig. 10, which was created as follows. We took the six lines for $\eta = 2$ from Fig. 9, and for each of them we computed the slope

15

of the line as a function of the horizontal coordinate in the figure, $\log_{10} t$. To compute this slope, we took each pair of adjacent points on the line and found the slope of the straight line connecting these points. The distance between two consecutive peaks in Fig. 9 is $|\log_{10} \sigma_{\mathrm{G}}|$; more interestingly, as $\log_{10} t$ becomes more negative, the lines tend to the same wavy line, until all lines reach saturation around $\log_{10} t \approx -4.5$.

4.4 Global Hölder regularities – numerical results

Table 1 summarizes our numerical results. The first column gives the map V used in the numerical computations (for the six functions V given by (16)–(21)). In the other columns we give the the values of the (global) Hölder exponent κ of the function R (representing the invariant circle as a graph in the (θ, r)-plane), the advance map g, the conjugacy h and its inverse, h^{-1}, coming from the (dynamics on) the golden critical invariant circle of the corresponding area-preserving twist map F. The notations used are the following: 1.85(15) stands for 1.85 ± 0.15, and 0.726(3) for 0.726 ± 0.003. Note that within the numerical error, $\kappa(R) = \kappa(g)$, as expected.

We also computed the Hölder regularities of all big conjugacies H between each of the six functions h_1, ..., h_6 (coming from V_1, ..., V_6) with all other h_j's. We applied the CLP method to find that the regularity of all thirty functions H studied is

$$\kappa(H) = 1.80 \pm 0.15 \ . \tag{22}$$

5 Discussion and conclusion

In Sections 5.1 and 5.2 we point out some relationships between our results and previous studies related to universal scaling factors and singular measures. In the final Section 5.3, we recapitulate our findings.

5.1 Hölder regularity and scaling factors

Here we will explain how the scaling of the distances of closest returns of the iterates of a point gives bounds on the Hölder regularity of some of the functions we study. Our analysis here is reminiscent of the analysis in [4, Sec. 8.2].

We start by recalling the crucial observation of Kadanoff and Shenker [1, 2] (see also [15, Sec. 4.4]) of the existence of universal scalings in the distribution of the iterates of the Taylor-Chirikov map on the critical invariant circle γ in neighborhoods of certain points of γ. Let $\theta_{\mathrm{rar}} \in \mathbb{T}$ stand for the value around which the iterates of the function g are most rarefied (in our notations $\theta_{\mathrm{rar}} = \frac{1}{2}$, while in [2] $\theta_{\mathrm{rar}} = 0$). Let $\theta_{\mathrm{den}} \in \mathbb{T}$ stand for the value around which the iterates of the function g are most dense (in our notations $\theta_{\mathrm{rar}} = 0$, while in [2] it is $\theta_{\mathrm{rar}} = \frac{1}{2}$). Since by Theorem 2.2 the function R is Lipschitz, around the points $(\theta_{\mathrm{rar}}, R(\theta_{\mathrm{rar}}))$ and $(\theta_{\mathrm{den}}, R(\theta_{\mathrm{den}}))$, the iterates of any point on γ under F are most rarefied, resp. dense. Shenker and Kadanoff found that the critical invariant circle in a neighborhood

of θ_{rar} is asymptotically invariant under simultaneous scalings in both θ- and r-directions, with scaling factors

$$\alpha_0 \approx -1.414836 \ \ (\text{in } \theta) \ , \qquad \beta_0 \approx -3.0668882 \ \ (\text{in } r)$$

(see also the bounds on these values in Stirnemann [36]). This implies that, for large n,

$$\frac{g^{Q_{n+1}}(\theta_{\text{rar}}) - \theta_{\text{rar}}}{g^{Q_n}(\theta_{\text{rar}}) - \theta_{\text{rar}}} \approx \alpha_0^{-1} \ , \qquad \frac{R(g^{Q_{n+1}}(\theta_{\text{rar}})) - R(\theta_{\text{rar}})}{R(g^{Q_n}(\theta_{\text{rar}})) - R(\theta_{\text{rar}})} \approx \beta_0^{-1} \ . \tag{23}$$

The scaling around θ_{den} is a bit more complicated – it is called "step-3" scaling for obvious reasons:

$$\frac{g^{Q_{n+3}}(\theta_{\text{den}}) - \theta_{\text{den}}}{g^{Q_n}(\theta_{\text{den}}) - \theta_{\text{den}}} \approx \alpha_3^{-1} \ , \qquad \frac{R(g^{Q_{n+3}}(\theta_{\text{den}})) - R(\theta_{\text{den}})}{R(g^{Q_n}(\theta_{\text{den}})) - R(\theta_{\text{den}})} \approx \beta_3^{-1} \ , \tag{24}$$

where the "step-3" scaling factors are

$$\alpha_3 \approx -4.84581 \ \ (\text{in } \theta) \ , \qquad \beta_3 \approx -16.8597 \ \ (\text{in } r) \ .$$

To understand heuristically why these scalings give restrictions on the Hölder regularity of R, set $\Delta\theta := g^{Q_{n+1}}(\theta_{\text{rar}}) - \theta_{\text{rar}}$, $\Delta r := R(g^{Q_{n+1}}(\theta_{\text{rar}})) - R(\theta_{\text{rar}})$ for some large value of n. Then if the local Hölder exponent of R at $\theta = \theta_{\text{rar}}$ is κ, we will have $|\Delta r| \sim |\Delta\theta|^\kappa$. If the graph of R is asymptotically invariant around $(\theta_{\text{rar}}, R(\theta_{\text{rar}}))$ with respect to the scalings (23), we will have $|\beta_0 \Delta r| \sim |\alpha_0 \Delta\theta|^\kappa$. "Dividing out" the last two relationships, we obtain $|\beta_0| \sim |\alpha_0|^\kappa$, i.e., $\kappa \sim \frac{\log|\beta_0|}{\log|\alpha_0|}$. This argument (which can easily be made rigorous) implies that the (global) Hölder exponent of R does not exceed $\frac{\log|\beta_0|}{\log|\alpha_0|} \approx 3.22945$. The scaling (24) yields a tighter bound on the Hölder regularity of R:

$$\kappa(R) \leq \frac{\log|\beta_3|}{\log|\alpha_3|} \approx 1.7901 \ . \tag{25}$$

Note that the fact that the scaling (24) is "step-3" (as opposed to "step-1") is irrelevant for the bounds on the Hölder regularity.

To obtain bounds on $\kappa(h)$ and $\kappa(h^{-1})$, we use Lemma 8.1 from [4], which says that if the function h conjugates f_1 and f_2, $h \circ f_1 = f_2 \circ h$, and if for some sequence of positive integers Q_n the functions f_j ($j = 1, 2$) behave in a neighborhood of the fixed point $\theta_{\text{fix}} = h(\theta_{\text{fix}})$ of h as follows:

$$f_j^{Q_n}(\theta_{\text{fix}}) = \theta_{\text{fix}} + C_j \eta_j^{-n} + o(\eta_j^{-n})$$

for some constants η_j and C_j, then $\kappa(h) \leq \frac{\log|\eta_2|}{\log|\eta_1|}$. Applying this to the definition of h and using the well-known fact that $(Q_n \sigma_{\text{G}}) \mod 1 \leq C\sigma_{\text{G}}^n$, we obtain the bounds

$$\kappa(h) \leq \frac{\log|\alpha_0^{-1}|}{\log|\sigma_{\text{G}}|} \approx 0.721125 \ , \qquad \kappa(h^{-1}) \leq \frac{\log|\sigma_{\text{G}}^3|}{\log|\alpha_3^{-1}|} \approx 0.91478 \ . \tag{26}$$

A comparison with Table 1 suggests that these bounds are saturated.

17

5.2 Conjugacies and singular measures

The functions whose Hölder regularity we study are defined through high iterates of maps. For example, the graph of the function R defined by (4) is nothing but the the critical invariant circle γ of F which is is filled densely by the iterates $F^n(\theta_0, r_0)$ of some point $(\theta_0, r_0) \in \gamma$. Here we discuss how some characterizations of the singularities in the distribution of the iterates of F on γ are related to the Hölder regularity of some of the functions considered.

Hentschel and Procaccia [37] pointed out the importance of the *generalized (Rényi) dimensions* $D(q)$ of a singular measure for dynamical systems; these quantities have been defined previously in the context of probability theory by Rényi [38]. Halsey et al in their seminal paper [3] related heuristically the Rényi dimension of a singular measure to the *spectrum of singularities* $f(\alpha)$. We recall that $f(\alpha)$ is the Hausdorff dimension of the set E_α of points where the measure has singularity of strength α. The spectrum $f(\alpha)$ is a function supported on the interval $[\alpha_{\min}, \alpha_{\max}]$, where $\alpha_{\min} = D(\infty)$, resp. $\alpha_{\max} = D(-\infty)$, describe the scaling behavior of the measure in the region where the measure is most dense, resp. most rarefied.

Let (θ_0, r_0) be an arbitrary point on the critical invariant circle γ of the area-preserving twist map F. Then the distribution of the iterates in a very long orbit, $\{F^n(\theta_0, r_0)\}_{n=0}^{K}$, approaches as $K \to \infty$ the "density" of the measure on γ that is invariant with respect of the restriction of the map F onto γ. (We put "density" is quotation marks because for singular measures this is not a function, but a set of Dirac δ-distributions.) This invariant measure on γ induces an invariant measure μ_g of the map g on $\mathbb{T}$. It is easy to see that (7) implies that

$$h^{-1}(\theta) = \int_0^\theta d\mu_g$$

(for an appropriately chosen ζ in the redefinition of h as in Sec. 2.5). This relationship implies that the spectrum of singularities $f(\alpha)$ of the measure μ_g is the same as the *Hölder spectrum* $f_{\mathrm{H}}(\alpha)$ of the function h^{-1}. By definition, $f_{\mathrm{H}}(\alpha)$ is the Hausdorff dimension of the set where the local Hölder exponent of the function is equal to α; for a readable account we refer the reader to Jaffard [39]. The (global) Hölder regularity $\kappa(\phi)$ of a function ϕ is equal to the lowest end, $\alpha_{\min}$, of the support of the Hölder spectrum, $f_{\mathrm{H}}(\alpha)$, of ϕ.

Osbaldestin and Sarkis [40] applied the method of [3] to determine numerically the functions $f(\alpha)$ and $D(q)$ of the invariant measure μ_g coming from the distribution of iterates of the Taylor-Chirikov map F on the golden invariant circle. They found that

$$\alpha_{\min} = D(\infty) \approx 0.915 \,, \qquad \alpha_{\max} = D(-\infty) \approx 1.387 \approx \frac{1}{0.720} \,.$$

Comparing with the values in Table 1, the reader should recognize that their $\alpha_{\min}$ is nothing but our $\kappa(h^{-1})$, while $\alpha_{\min}$ is equal to the inverse of the regularity of the conjugacy h.

Burić et al [41, 42] studied numerically the Taylor-Chirikov map and the map (1) with $V(\theta) = \frac{1}{2}\sin 2\pi\theta + \frac{1}{4}\sin 4\pi\theta$, for rotation numbers with continued fraction expansions of the form $[S, 1^\infty] := [S, 1, 1, 1, \ldots], [S, 2^\infty], [S, 3^\infty], [S, 4^\infty]$, where S stands for some short string of positive integers. They found that $f(\alpha)$ and $D(q)$ depend only on the tail but do not

18

depend on the initial part S as well as on whether the Taylor-Chirikov map or the other map was used in their numerics.

Other papers related to numerical computations of singular measures on critical invariant circles of area-preserving twist maps are Shi and Hu [43, 44], where the methods of [3] were used, and Hunt et al [45], where the authors used the thermodynamic formalism developed in [46] to compute the information dimension $D(1)$ of the standard map for different rotation numbers.

5.3   Conclusion

We computed accurately the golden critical invariant circles for six twist maps of the form (1) and the global Hölder regularity κ of some functions related to the dynamics on these circles. Our numerical experiments lend credibility to Conjectures 2.3, 2.4 and 2.5 concerning the universality of the regularities of the functions R, g, h, h^{-1} and H (see Table 1 and (22)). Yamaguchi and Tanikawa [47] found numerically that the golden invariant circle (given by the function R) of the Taylor-Chirikov map is differentiable but R' is not of bounded variation; our studies significantly narrow the numerical bounds on $\kappa(R)$ for this and for other maps.

Our results seem to indicate that the regularities of R, h, and h^{-1} saturate the upper bounds (25) and (26) coming from previous studies of scaling exponents.

Our finding that $\kappa(H)$ is greater than $\kappa(h)$ and $\kappa(h^{-1})$ by a comfortable margin (cf. Conjecture 2.6) has an interesting consequence. As discussed in Sec. 5.2, the Hölder regularity of h and h^{-1} is different at different points, and for each $\alpha \in (\alpha_{\min}, \alpha_{\max})$, the set E_α (where the pointwise Hölder exponent of h^{-1} is α) has Hausdorff dimension $f_H(\alpha)$ strictly between 0 and 1. Previous numerical studies indicated that $f_H(\alpha)$ are the same for different maps F. Our finding shows that the "irregularities" of functions h coming from different maps F are interspersed in the same way in $[0, 1]$ for all twist maps studied. Note that this does not mean that for a certain value of α the sets E_α are *the same* for different F in the same universality class – only the way all sets E_α for different α are interwoven is universal.

It would be interesting to apply wavelet-maxima methods for pointwise regularity [48, 49] (see also the rigorous analysis in [39]) to the problem studied in this paper and to compare the results of the wavelet analysis with the results about the singular invariant measures.

As a by-product of our studies, we have computed millions of Fourier coefficients of the functions h, and noticed some self-similarity properties that to the best of our knowledge have not been observed before. Presently we are working on understanding these properties.

19

Acknowledgments

References

[1] L. Kadanoff, "Scaling for a critical Kolmogorov-Arnold-Moser trajectory", *Phys. Rev. Lett.* **47** (1981), 1641–1643.

[2] S. Shenker and L.P. Kadanoff, "Critical behavior on a KAM surface: I. Empirical results", *J. Stat. Phys.* **27** (1982), 631–656.

[3] T. C. Halsey, M. H. Jensen, L. P. Kadanoff, I. Procaccia, B. I. Shraiman, "Fractal measures and their singularities: The characterization of strange sets", *Phys. Rev. A* **33** (1986), 1141–1151, reprinted in [51, pp. 540–550].

[4] R. de la Llave and N. Petrov, "Regularity of conjugacies between critical circles maps: An experimental study", *Experiment. Math.* **11** (2002), 219–241.

[5] C. Tresser and P. Coullet, "Itérations d'endomorphismes et groupe de renormalisation", *C. R. Acad. Sci. Paris Sér. A-B* **287** (1978), A577–A580.

[6] M. J. Feigenbaum, "Quantitative universality for a class of nonlinear transformations", *J. Stat. Phys.* **19** (1978), 25–52.

[7] M. J. Feigenbaum, "The universal metric properties of nonlinear transformations", *J. Stat. Phys.* **21** (1979), 669–706, reprinted in [51, pp. 207–244].

[8] S. Shenker, "Scaling behavior in a map of a circle onto itself: empirical results", *Phys. D* **5** (1982), 405–411, reprinted in [51, pp. 405–411].

[9] P. Collet, J. P. Eckmann and O. E. Lanford, III, "Universal properties of maps on an interval", *Comm. Math. Phys.* **76** (1981), 211–254.

[10] M. J. Feigenbaum, L. P. Kadanoff, and S. J. Shenker, "Quasiperiodicity in dissipative systems: a renormalization group analysis", *Phys. D* **5** (1982), 370–386.

[11] S. Ostlund, D. Rand, J. Sethna, and E. Siggia, "Universal properties of the transition from quasiperiodicity to chaos in dissipative systems", *Phys. D* **8** (1983), 303–342.

[12] R. S. MacKay, "A renormalisation approach to invariant circles in area preserving twist maps", *Phys. D* **7** (1983), 283–300, reprinted in [53, pp. 462–479].

[13] J. D. Meiss, "Symplectic maps, variational principles, and transport", *Rev. Modern Phys.* **64** (1992), 795–848.

[14] C. Golé, *Symplectic Twist Maps*, World Scientific, 2001.

[15] R. S. MacKay, "Renormalization in Area Preserving Maps", *PhD Thesis*, Princeton University, 1982; published with notes as R. S. MacKay, *Renormalization in Area-Preserving Maps*, World Scientific, Singapore, 1993.

[16] G. D. Birkhoff, "Surface transformations and their dynamical applications", *Acta Math.* **43** (1920), 1–119, reprinted in [52, pp. 111–229].

[17] J. Mather, "Nonexistence of invariant circles", *Ergodic Theory Dynam. Systems* **4** (1984), 301-309, reprinted in [53, pp. 395–403].

[18] J. J. Mather and G. Forni, "Action minimizing orbits in Hamiltonian systems", *Transition to Chaos in Classical and Quantum Mechanics (Montecatini Terme, 1991)*, J. Bellissard et al, Eds., Springer, Berlin, (1994), 92–186.

[19] A. Ya. Khinchin, *Continued Fractions*, Dover, Mineola, NY, 1997.

[20] R. S. MacKay and I. C. Percival, "Converse KAM: theory and practice", *Comm. Math. Phys.* **98** (1985), 469–512.

[21] I. Jungreis, "A method for proving that monotone twist maps have no invariant circles", *Ergodic Theory Dynam. Systems* **11** (1991), 79–84.

[22] R. DeVogelaere, "On the structure of symmetric periodic solutions of conservative systems, with applications", In *Contributions to the Theory of Nonlinear Oscillations*, S. Lefschetz (Ed.), Princeton University Press, 1958, pp. 53–84.

[23] J. M. Greene, "A method for determining a stochastic transition", *J. Math. Phys.* **20** (1979), 1183–1201, reprinted in [53, pp. 419–437].

[24] A. Apte, R. de la Llave and N. P. Petrov, "Regularity of critical invariant circles of the standard nontwist map", *Nonlinearity* **18** (2005), 1173–1187.

[25] J. A. Ketoja, "Renormalisation in a circle map with two inflection points", *Phys. D* **55** (1992), 45–68.

[26] J. A. Ketoja and R. S. MacKay, "Rotationally-ordered periodic orbits for multiharmonic area-preserving twist maps", *Phys. D* **73** (1994), 388–398.

[27] C. Falcolini and R. de la Llave, "Numerical calculation of domains of analyticity perturbation theories in the presence of small divisors", *J. Stat. Phys.* **67** (1992), 645–666.

[28] R. de la Llave and A. Olvera, "The obstruction criterion for non-existence of invariant circles and renormalization", *Nonlinearity* **19** (2006) 1907–1937.

[29] R. de la Llave and R. P. Schafer, "Rigidity properties of one dimensional expanding maps and applications to renormalization", Manuscript, 1996.

[30] G. D. Birkhoff, "An extension of Poincaré's last geometric theorem", *Acta Math.* **47** (1925), 297–311, reprinted in [52, pp. 252–266].

[31] A. Katok and B. Hasselblatt, *Introduction to the Modern Theory of Dynamical Systems*, Cambridge University Press, Cambridge, 1995.

[32] A. Olvera and C. Simó, "An obstruction method for the destruction of invariant curves", *Phys. D* **26** (1987), 181–192.

[33] C. Falcolini and R. de la Llave, "A rigorous partial justification of Greene's criterion", *J. Stat. Phys.* **67** (1992), 609–643.

[34] T. Carletti, "The 1/2-complex Bruno function and the Yoccoz function: a numerical study of the Marmi-Moussa-Yoccoz conjecture", *Experiment. Math.* **12** (2003), 491–506.

[35] E. Stein, *Singular Integrals and Differentiability Properties of Functions*, Princeton University Press, Princeton, 1970.

[36] A. Stirnemann, "Towards an existence proof of MacKay's fixed point", *Commun. Math. Phys.* **188** (1997), 723–735.

[37] H. G. E. Hentschel and I. Procaccia, "The infinite number of generalized dimensions of fractals and strange attractors", *Phys. D* **8** (1983), 435–444.

[38] A. Rényi, "On measures of entropy and information", in *Proceedings of the Fourth Berkeley Symposium on Mathematical Statistics and Probability, University of California, June 20–July 30, 1960, Vol I*, University of California Press, Berkeley, 1961, pp. 547–561.

[39] S. Jaffard, "Multifractal formalism for functions. I. Results valid for all functions. II. Self-similar functions", *SIAM J. Math. Anal.* **28** (1997), 944–970, 971–998.

[40] A. H. Osbaldestin and M. Y. Sarkis, "Singularity spectrum of a critical KAM torus", *J. Phys. A* **20** (1987), L953–L958.

[41] N. Burić, M. Mudrinić and K. Todorović, "Equivalent classes of critical circles", *J. Phys. A* **30** (1997), L161–L165.

[42] N. Burić, M. Mudrinić and K. Todorović, "Universal scaling of critical quasiperiodic orbits in a class of twist maps", *J. Phys. A* **39** (1998), 7848–7854.

[43] J. Shi and B. Hu, "Crossover phenomena in the multifractal behavior of invariant circles", *Phys. Lett. A* **156** (1991), 267–271.

[44] B. Hu and J. Shi, "Nonanalytic twist maps and Frenkel-Kontorova model", *Phys. D* **71** (1994), 23–38.

[45] B. R. Hunt, K. M. Khanin, Ya. G. Sinai, and J. A. Yorke, "Fractal properties of critical invariant curves", *J. Stat. Phys.* **85** (1996), 261–276.

[46] E. B. Vul, Ya. G. Sinai, and K. M. Khanin, "Feigenbaum universality and thermodynamic formalism", *Russian Math. Surveys* **39** (1984), 1–40, reprinted in [51, pp. 491–530].

[47] Y. Yamaguchi and K. Tanikawa, "A remark on the smoothness of critical KAM curves in the standard mapping", *Prog. Theor. Phys.* **101** (1999), 1–24.

[48] A. Arneodo, E. Bacry and J. F. Muzy, "The thermodynamics of fractals revisited with wavelets", *Phys. A* **213** (1995), 232–275.

[49] J. F. Muzy, E. Bacry and A. Arneodo, "The multifractal formalism revisited with wavelets", *Internat. J. Bifur. Chaos Appl. Sci. Engrg.* **4** (1994), 245–302.

[50] The Grace team, Grace homepage. `http://plasma-gate.weizmann.ac.il/Grace/`.

[51] P. Cvitanović, *Universality in Chaos*, IOP Publishing, Bristol, 1989.

[52] G. D. Birkhoff, *Collected Works, Vol II*, Dover, New York, 1968.

[53] R. S. MacKay and J. D. Meiss, *Hamiltonian Dynamical Systems*, Adam Hilger, Bristol, 1993.

Tables

F with:	$\kappa(R)$	$\kappa(g)$	$\kappa(h)$	$\kappa(h^{-1})$
V_1	1.83(9)	1.83(9)	0.722(1)	0.92(1)
V_2	1.79(6)	1.75(9)	0.721(1)	0.92(1)
V_3	1.83(4)	1.84(3)	0.724(2)	0.93(2)
V_4	1.86(8)	1.86(8)	0.722(1)	0.92(1)
V_5	1.85(5)	1.85(5)	0.724(2)	0.93(1)
V_6	1.85(15)	1.88(12)	0.726(3)	0.93(2)

Table 1: Regularities of the functions R, g, h, and h^{-1} for the golden critical invariant circles of different maps F.

Figure captions

Caption to Figure 1:
Critical invariant circles, $r = R(\theta)$, of the maps corresponding to the maps V_1, V_2, ..., V_6 given by (16)–(21) (V_1 = thin solid line, V_2 = thick solid line, V_3 = dotted line, V_4 = thin dashed line, V_5 = thick dashed line, V_6 = dot-dashed line).

Caption to Figure 2:
"Periodized" advance maps $g - \mathrm{Id}$ (notation same as in Fig. 1).

Caption to Figure 3:
"Periodized" conjugacies $h - \mathrm{Id}$ (notation same as in Fig. 1).

Caption to Figure 4:
"Periodized" inverse conjugacies $h^{-1} - \mathrm{Id}$ (notation same as in Fig. 1).

Caption to Figure 5:
Zooming in the graph of the function $h - \mathrm{Id}$ corresponding to the map V_2 (17).

Caption to Figure 6:
"Periodized" big conjugacies $H - \mathrm{Id}$.

Caption to Figure 7:
Plot of $\log_{10}\left|\left(\widehat{h - \mathrm{Id}}\right)_k\right|$ versus $\log_{10} k$, where h corresponds to the map F coming form the function V_3 (18).

Caption to Figure 8:
Plot of $\log_{10}\left|\left(\widehat{g - \mathrm{Id}}\right)_k\right|$ and $\log_{10}\left|\left(\widehat{h^{-1} - \mathrm{Id}}\right)_k\right|$ versus $\log_{10} k$, for the same map F as in Fig. 7. The impulses correspond to $(g - \mathrm{Id})$, and the dots above them to $(h^{-1} - \mathrm{Id})$.

Caption to Figure 9:
Plots of $\log_{10}\left\|\left(\frac{\partial}{\partial t}\right)^\eta e^{-t\sqrt{-\Delta}} K\right\|_{L^\infty(\mathbb{T})}$ versus $\log_{10} t$ for the functions $K = (h - \mathrm{Id})$ for the twist maps coming from V_1, ..., V_6, for $\eta = 2$ (shallowest lines), $\eta = 3$, and $\eta = 4$ (steepest lines).

Caption to Figure 10:
Slope of the lines on Fig. 9 as a function of $\log_{10} t$ (see the text). The notation is the same as in Fig. 1.
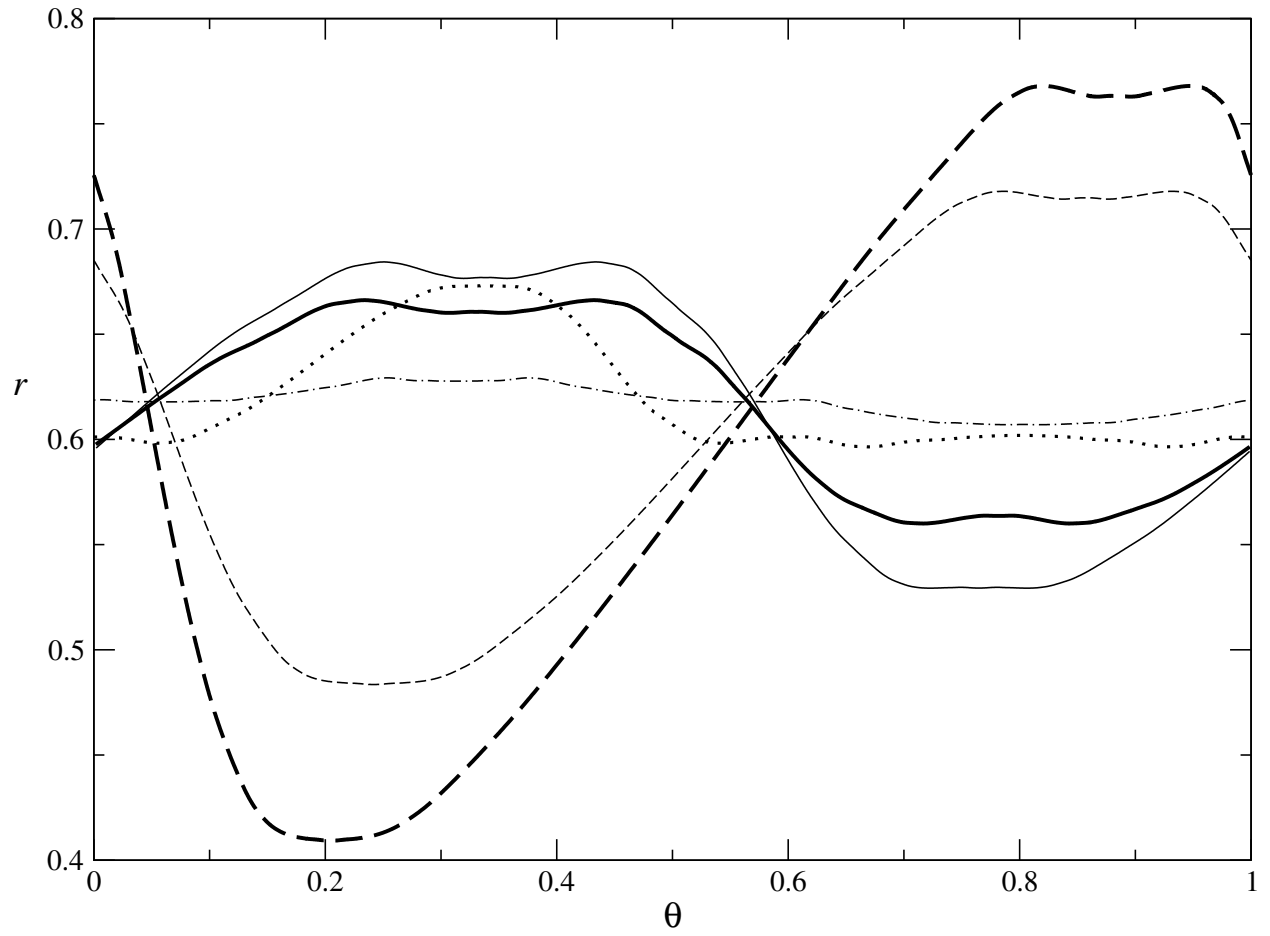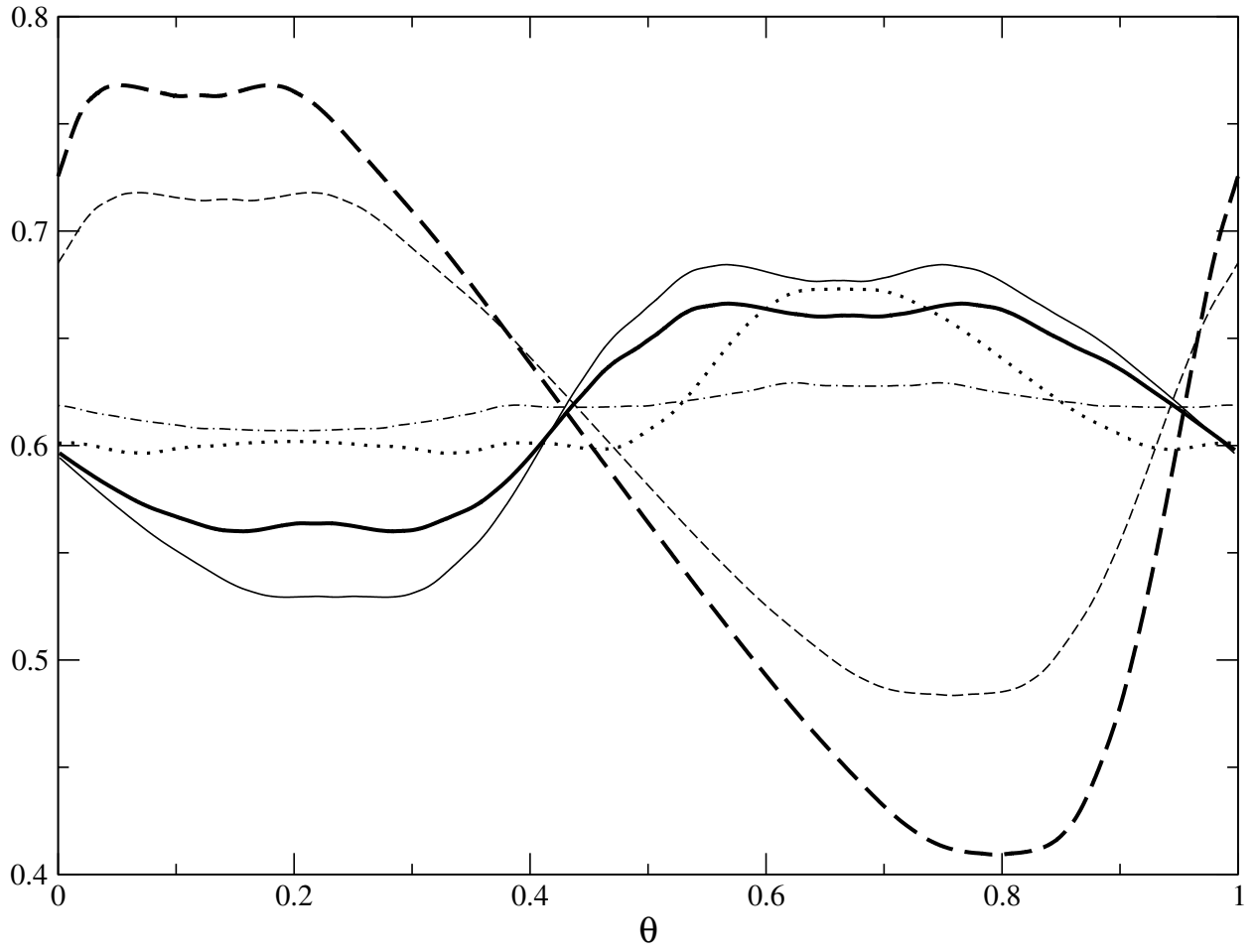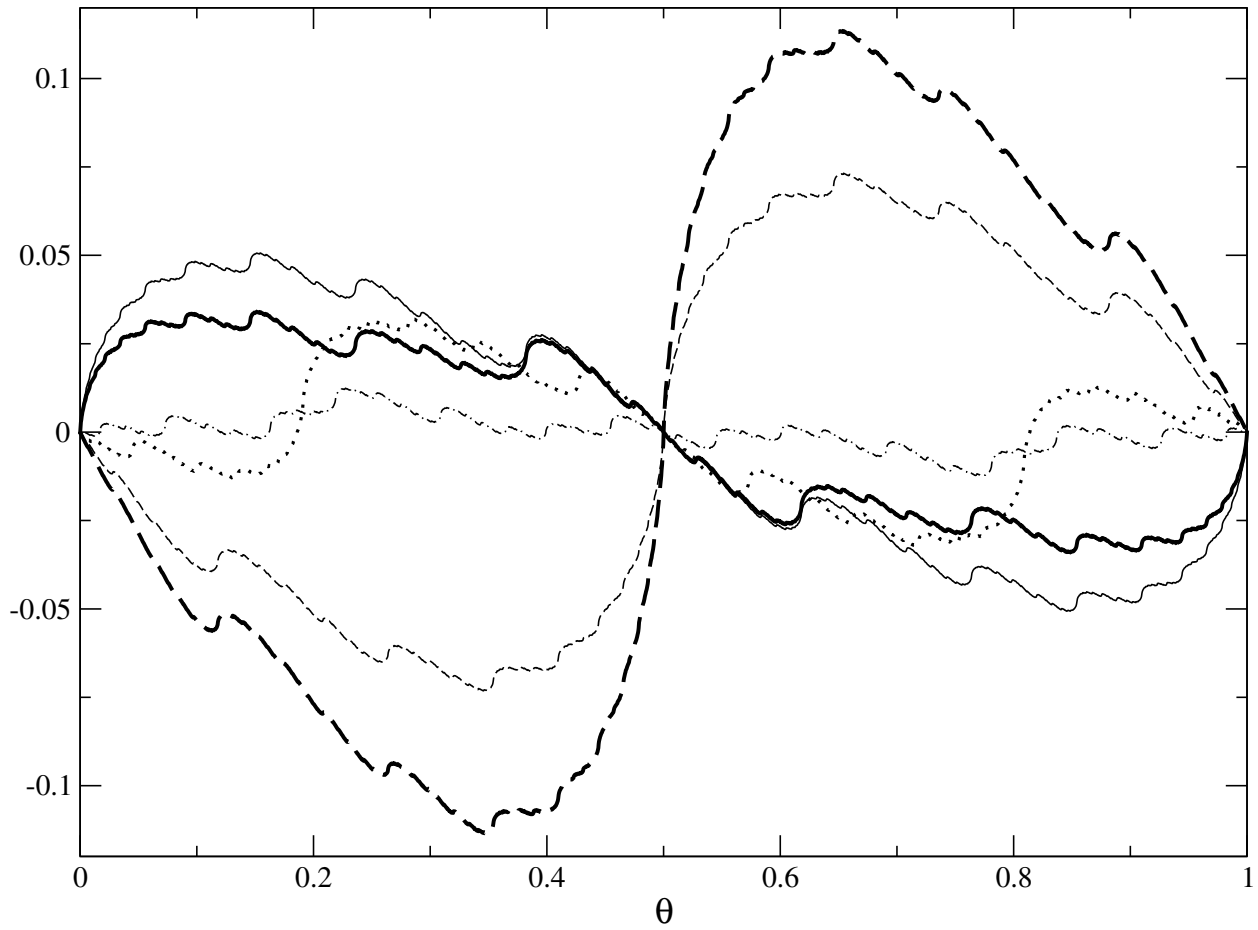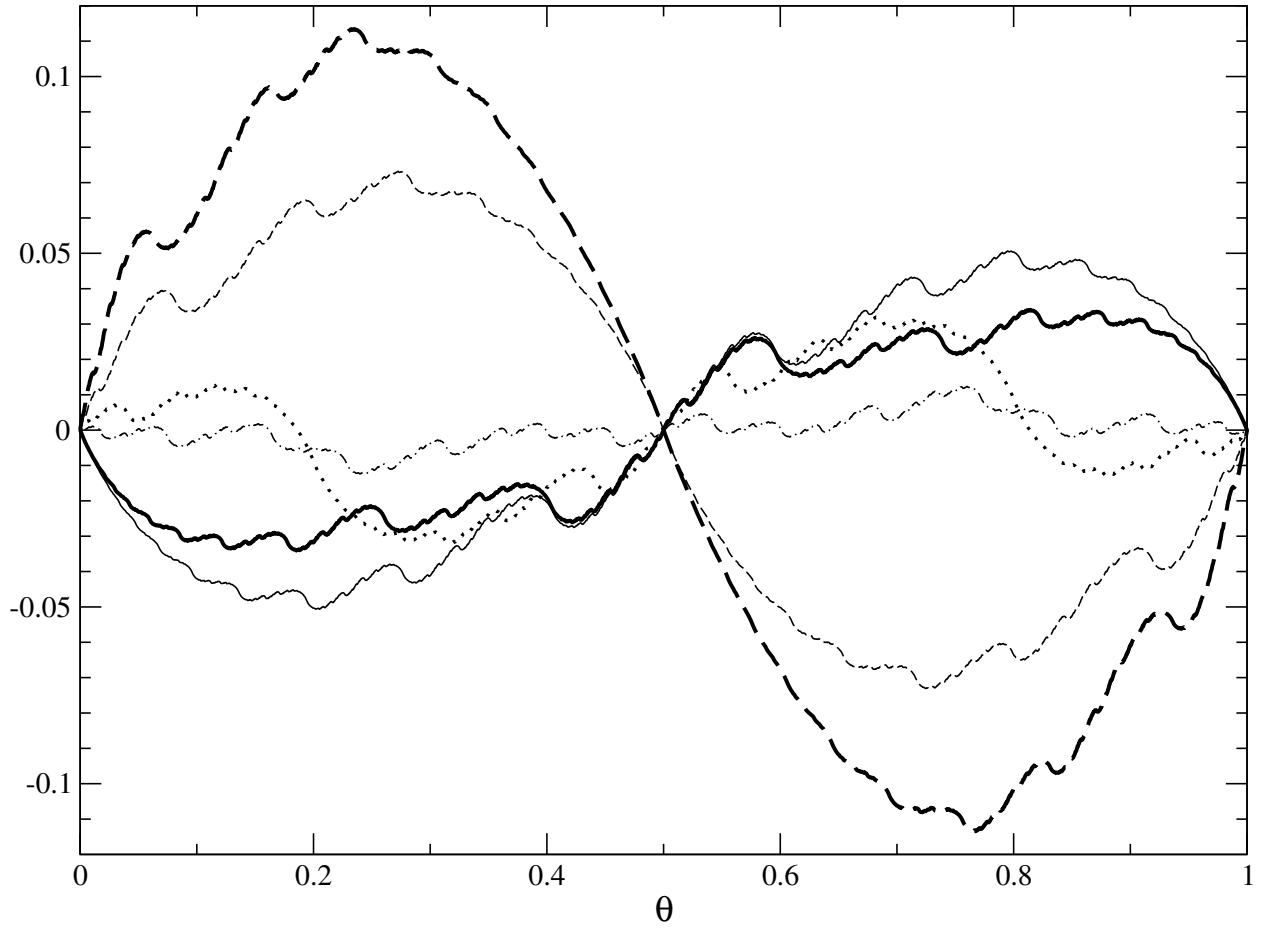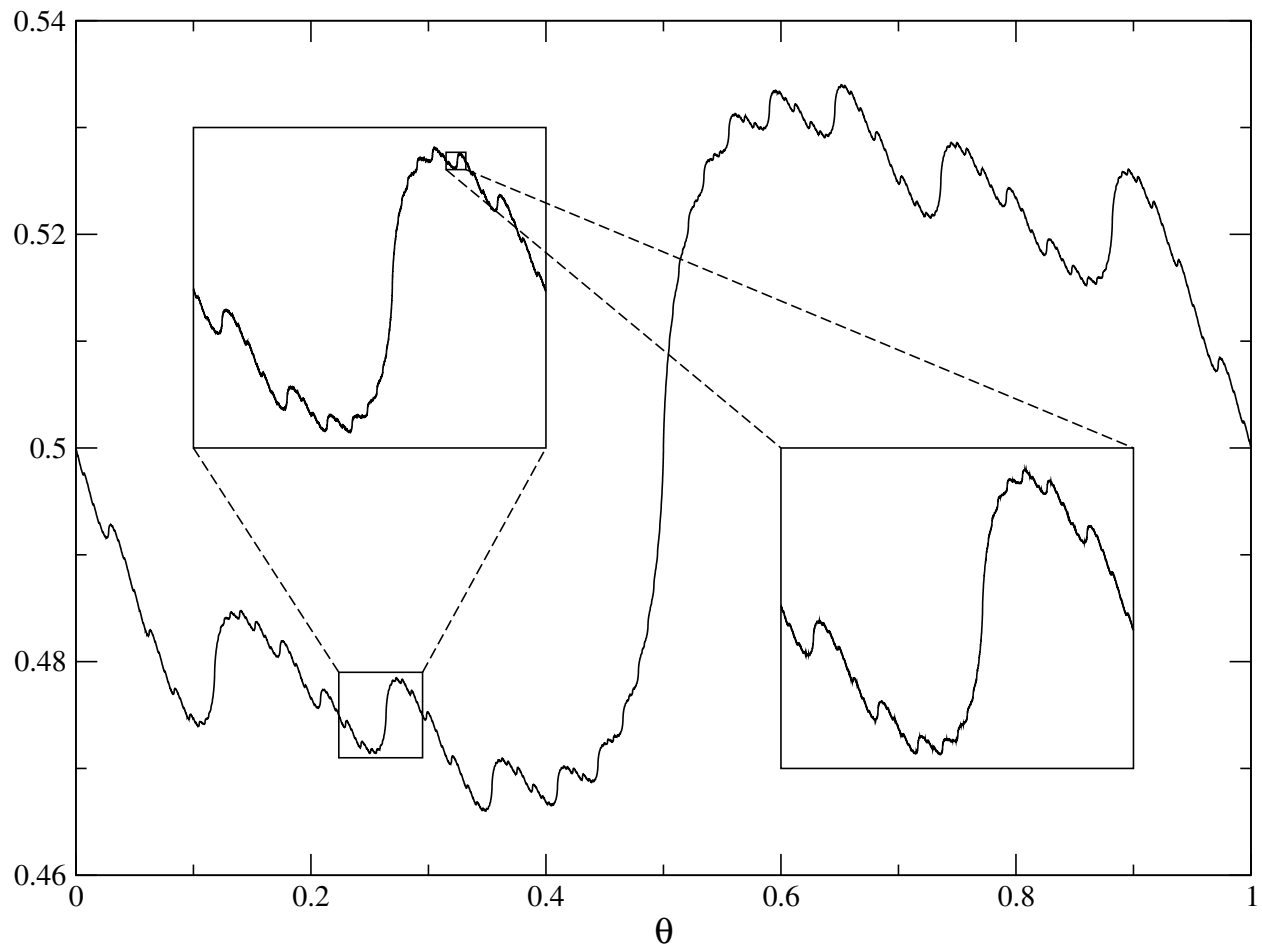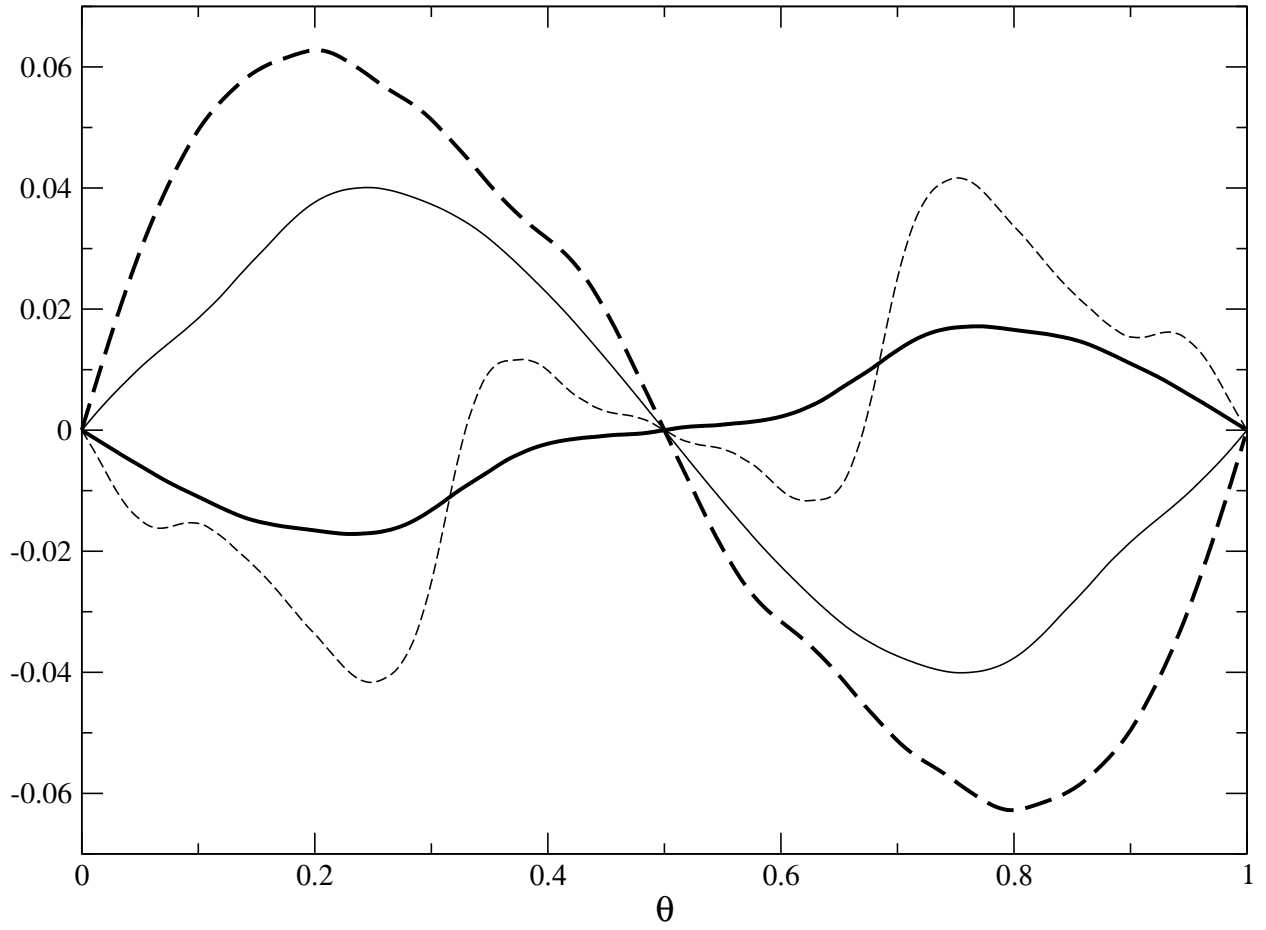
Figures

Figure 1:

Figure 2:

28

Figure 3:

Figure 4:

Figure 5:

Figure 6:
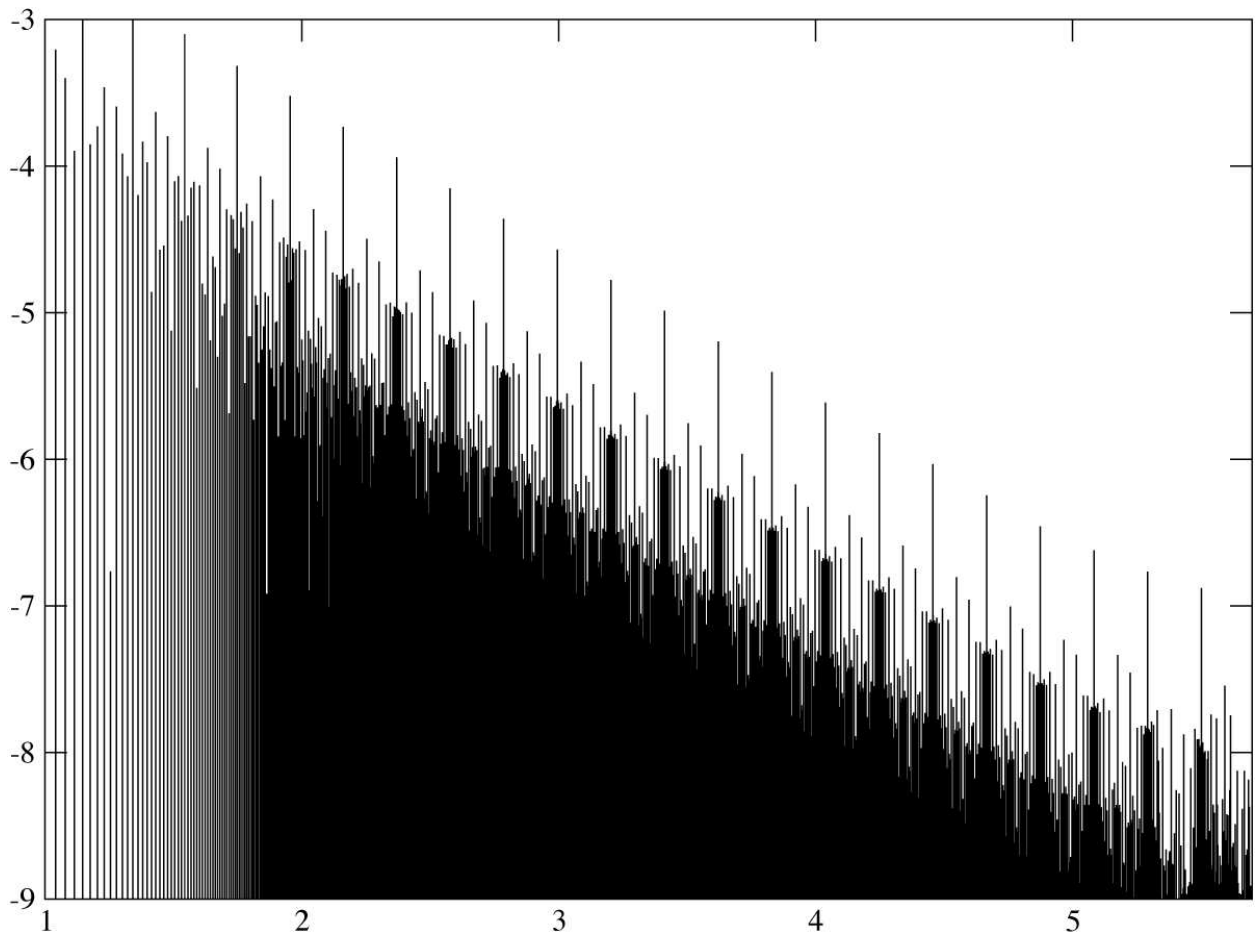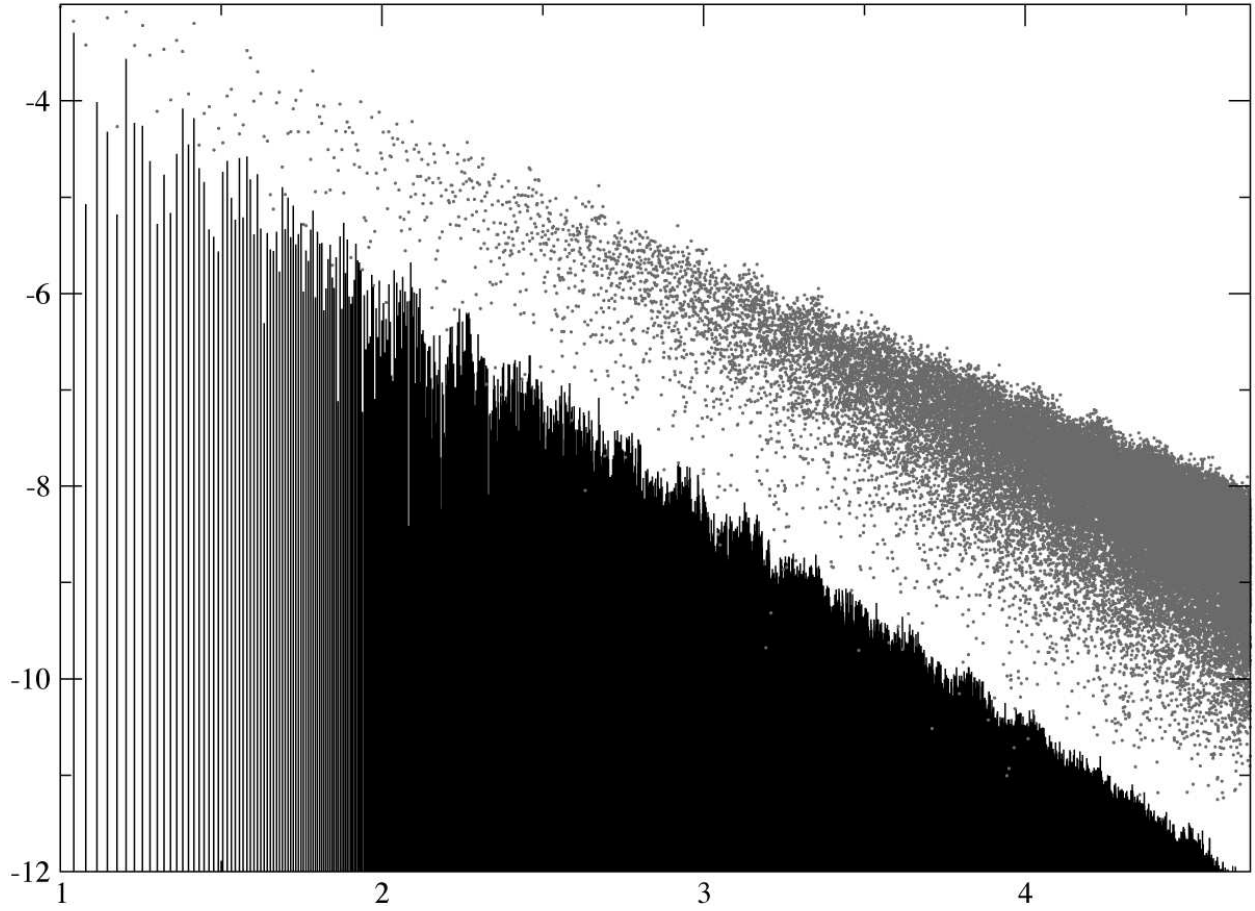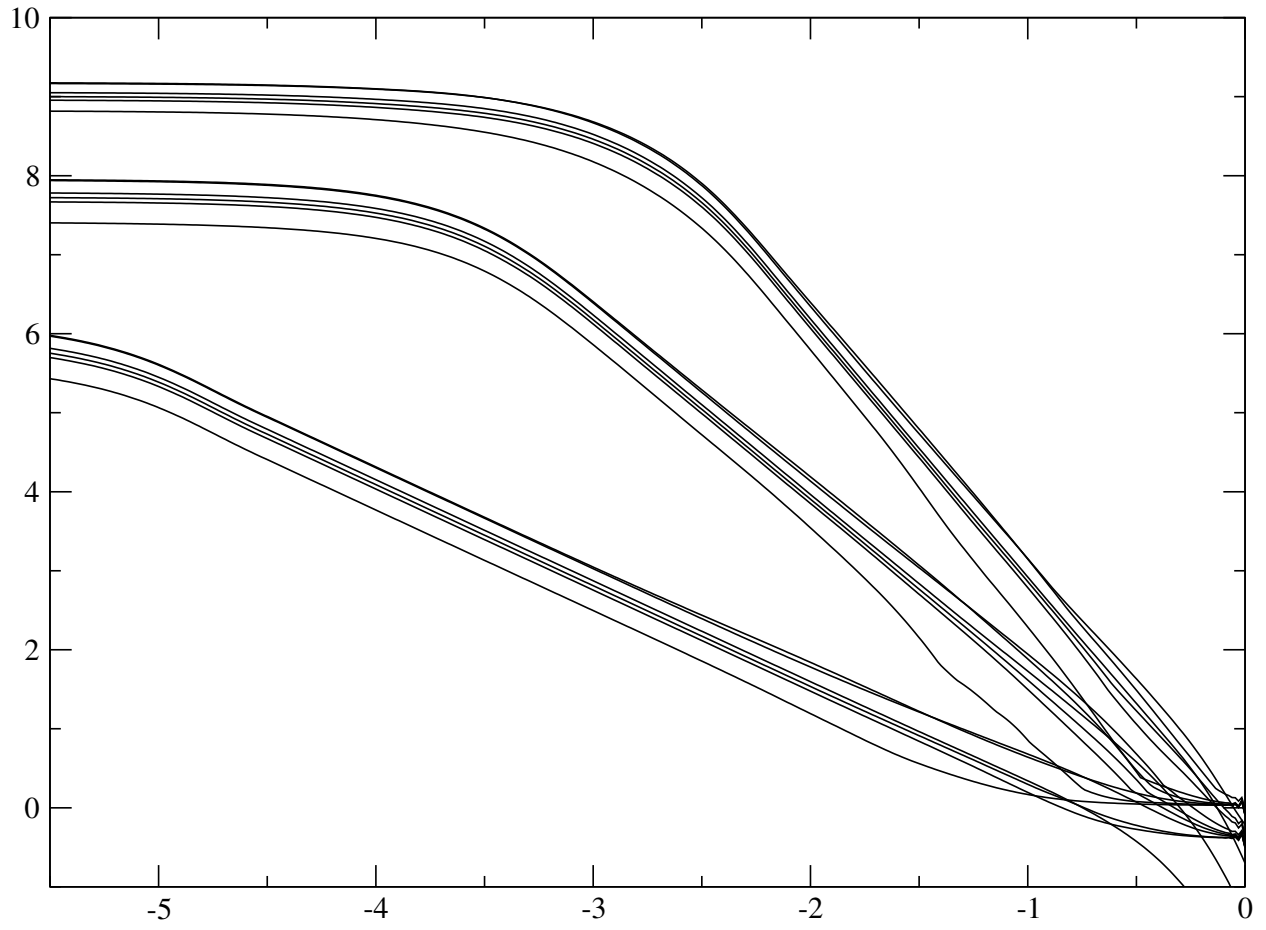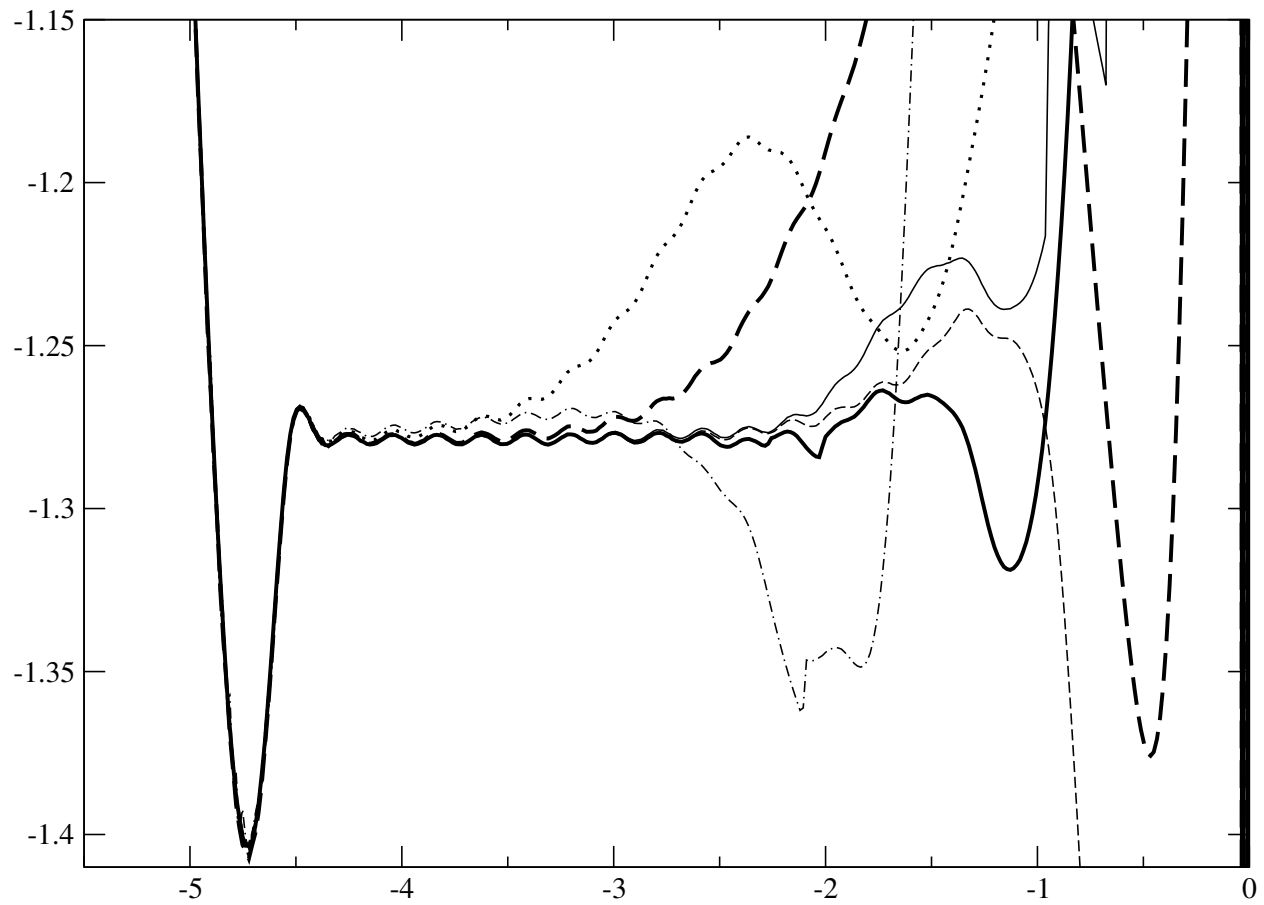
Figure 7:

Figure 8:

Figure 9:

35

Figure 10: